ULTRASOUND TREATMENT AS A NEW WAY FOR DEFECT ENGINEERING IN SEMICONDUCTOR MATERIALS AND DEVICES

Moisey K. Sheinkman, Nadezhda E. Korsunskaya, Sergey S. Ostapenko*

Institute of Semiconductor Physics
National Academy of Sciences of Ukraine
45 Prospect Nauky, Kyiv 252028, Ukraine
Phone/Fax: +380-44-2656340; E-mail: moishe@photel.semicond.kiev.ua

*Center for Microelectronics Research
University of South Florida
4202E Flower Avenue, Tampa, FL 33620, USA
Phone: (813) 974 203; FAX: (813) 974 3610; E-mail: ostapenk@eng.usf.edu

SUMMARY

UltraSound Treatment, UST, of semiconductors in many cases results in a stable improvement of material properties and device parameters and thus can be used in a defect engineering. The physical backgrounds of such effects as well as UST methods and apparatus are described.

1. INTRODUCTION

Discovered in the late 60's and extensively explored since 80's [1], the ultrasound stimulated processes in Ge, Si, and compound semiconductors attracted the attention of various research groups. It has been demonstrated that ultrasonic vibrations generated into crystal can stimulate numerous defect reactions and, as a consequence, benefit a design of electronic materials with improved and even superior characteristics. This new technological approach has become a powerful tool of the defect engineering to improve performance and reliability of microelectronics devices.

Ultrasonic processing of semiconductors and relevant mechanisms are referred to as UltraSound Treatment (hereafter the UST). UST effect is a stable improvement of material properties and device parameters after they being affected by the ultrasound. The UST method utilizes a fundamental concept in solids; it is based on a coupling of the ultrasonic vibrations with a system of point defects, both of impurity and native origin, interacting with the extended defects such as dislocations, grain boundaries, and precipitates to control their physical properties, and to improve defect related material parameters. Therefore, UST realizes a method of defect engineering in semiconductors to benefit a material quality. UST method is based on a solid and well understood physical concept. Crystal defects and their complexes can exist in a stable, unstable or metastable configuration. The bottomline of UST technology is that mechanical vibrations can "help" a system of crystal defects in reaching a favorable position which has the lowest total energy; therefore, this is the preferable, stable state. On the other hand, UST is a simple and intuitive approach. Many people experienced with a simple "ultrasound treatment" in their daily routine, may be without noticing it.

This article describes the UST method and apparatus, and also summarizes UST controlled defect reactions, relevant mechanisms, and application issues. Particular examples: dislocation gettering in II-VI semiconductors and enhanced hydrogenation in poly-Si thin films provide a deeper insight into specific UST mechanisms.

2. UST METHOD AND APPARATUS

Ultrasonic vibrations have to be delivered to a semiconductor materials or electronic device to perform UST processing. Three different techniques to generate ultrasonic vibrations are applicable.

1. The most general method utilizes an external source of the ultrasound, such as a resonance piezoelectric transducer. This UST technique has advantages of a non-contact processing in an active device region at the front surface of wafer and applicable for large-scale materials and devices, such as 8" Si-wafers and more than 12" flat-panel-displays. This UST approach is also compatible with conventional device processing's steps: deposition, annealing, doping, and passivation. A schematic of

0-7803-4432-4/98/$10.00

the UST unit - key element of large-scale UST station - is shown in Figure 1.

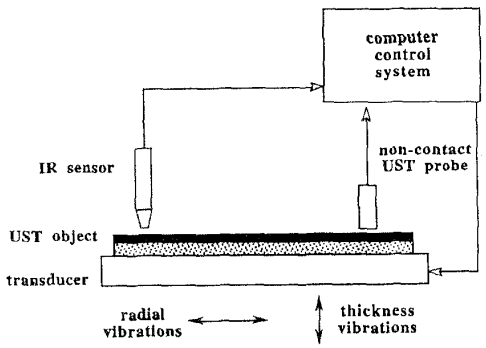

Figure 1. Schematic of ultrasound treatment unit for UST processing of semiconductor materials and devices.

Low-amplitude ultrasonic vibrations are generated into UST object: a semiconductor wafer, thin film on a substrate, or a microelectronics device using a piezoelectric transducer operating in a resonance vibration mode and coupled with UST object.

Typically, a circular transducer is driven by a generator and power amplifier adjusted to the first resonance of its radial or thickness vibrations. The resonance frequency varies from 20KHz to 100KHz for radial vibration mode and can be extended in MHz-range using thickness vibrations. This frequency depends on the transducer geometry, vibration mode, material of a piezoelectric transducer, and varies with UST temperature and amplitude. Adjusted to a resonance frequency, UST transducer generates a maximum ultrasonic amplitude which is quantified by a value of the acoustic strain. The amplitude of acoustic strain is a ratio of vibrating amplitude to a characteristic size of the transducer (e.g. diameter). In UST technique, the acoustic strain does not exceed typically 10^{-4} corresponding to the acoustic power of a few W/cm^2. The UST temperature can be stabilized from a room temperature to the Curie point of transducer (350°C for commercial PZT-5A piezoceramics). A sample has to be placed on a UST chuck composed of one or more UST transducers and tightly pressed against a chemically-polished transducer surface using a vacuum contact.

2. UST vibrations can be alternatively generated into material using the internal piezoelectric effect of a semiconductor. In this case, the ac voltage can be applied via electrodes oriented along specific crystallographic directions (e.g. along C axis in hexagonal-type crystal). The ac electric field generates intensive ultrasonic vibrations when its frequency (between 100KHz and 20MHz) is adjusted to the acoustic resonance of a sample. This method is limited to semiconductors with a high resistance possessing a noticeable piezoelectric constant (CdS, CdSe, $CdZnP_2$, and others). It also requires a special sample shaping in a form of the acoustic resonator.

3. Another UST approach is based on a pulsed laser absorption. The absorption in a crystal of a short nanosecond laser pulse (e.g. a ruby laser with a power density of the order 10^{12} W/cm^2) generates a set of ultrasonic pulses. These ultrasonic vibrations can be coupled with crystal defects and perform an effective UST processing. In this technique, laser density of power has to be carefully controlled to prevent the degradation of a material due to creation of new crystal defects.

3. FUNDAMENTAL: UST PHENOMENA AND MECHANISMS

Although UST effects in semiconductors are well documented, there are a limited number of conclusive results where a clear understanding of relevant physical mechanisms was achieved. Table I comprises a summary of UST mechanisms identified in various semiconductor materials. The key UST experiments, illustrating specific topics, will be discussed in detail.

UST mechanisms are tightly related to processes of point defect gettering. There are two general ways to achieve a high device yield and reliable device performance in IC technology.

The first one requires top-quality starting material which has to be processed further under an extremely clean fab environment. This is potentially a superior approach but at present is not a realistic one.

The second approach suggests the use of various defect engineering tools, particularly gettering and passivation to grow starting wafers with a moderate contamination level and to achieve a high-quality final product - the IC chip. According to a general gettering strategy, the gettering process is comprised of three consecutive steps:

1) release of a bound contamination impurity (Fe, Cu, Cr) introduced during wafer/device processing in a device region near the front surface of a wafer;

2) diffusion of released impurity toward the gettering sites (sinks) which are typically placed far away from the device region (e.g. at the back-side wafer surface);

3) capture of contamination atoms at crystallographic defects or binding them with

chemical elements at the gettering sites. Two particular gettering processes - relaxation gettering and segregation gettering - can be implemented. It was found that UST processing can positively affect each of three gettering steps: release, diffusion and capture as will be illustrated hereafter.

UST dissociation

Contamination of commercial Si wafers with iron, even at the level of 10^{11} cm^{-3}, is detrimental for IC manufacturing. Therefore, a sensitive technique was developed for in-line control of Fe-contamination. This technique utilizes a method of surface photovoltage (SPV) to measure minority carrier diffusion length in the bulk of a semiconductor [2]. Briefly, SPV is a non-contact, real-time method of quantitatively analyzing heavy metals in wafers. The technique uses light pulses directed onto the wafer to generate excess minority carriers. These carriers diffuse to the surface and change surface potential. A non-contact electrode placed above Si wafer surface senses the photovoltage which is measured as a function of the light penetration depth into bulk silicon. The shorter the diffusion length, or the higher a contamination, the faster photovoltage is decreased with increasing light penetration depth.

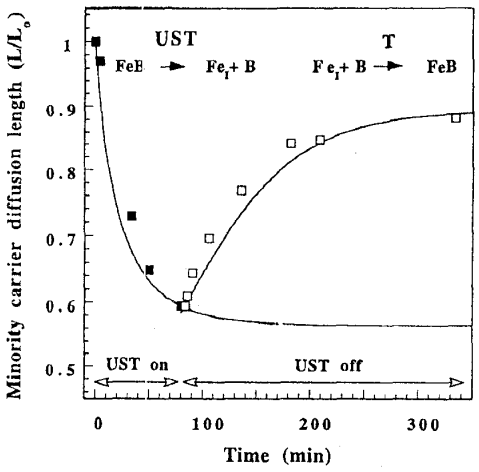

Figure 2. UST applied to p-type Cz-Si promotes breaking of Fe-B pairs. This process is monitored by a decrease of minority carrier diffusion length. After ultrasound is turned off Fe and B are paired again, accomplishing reversible dissociation/association process. UST breaking and pairing kinetics are measured at 75 °C.

For UST experiments, boron doped Cz-Si wafers were contaminated with iron at a concentration of 1.5×10^{14} cm^{-3}. This concentration was evaluated by means of an optical activation technique. At room temperature in p-type material, the Fe is paired with doping acceptors (B) forming stable up to 200°C nearest neighbor Fe-B pair. UST performed at temperatures below 100°C at 70kHz stimulates the process of Fe-B pair dissociation. This was controlled by reduction of minority carrier diffusion length measured with SPV technique as shown in Figure 2.

It is important that 200 °C annealing of Si is required for thermal dissociation of Fe-B pairs. The UST enhanced dissociation is followed by a pairing of Fe and B due to a colombic attraction of charged pair constituents and a fast diffusion of the interstitial Fe. Therefore, this UST triggered process is entirely reversible. This model case of Fe-B splitting under UST has the following explanation. A mobile Fe, bound with boron in the Fe-B pair, can exhibit a jumping from one interstitial position to a nearest equivalent one.

The jumping rate is strongly stimulated when the frequency, f, of the applied ultrasonic vibrations is close to the resonance of pair reorientation followed by the equation:

$$2\pi f = \nu_0 \exp(-U/kT) \qquad (1)$$

where ν_0 is the lattice phonon frequency (typically of the order 10^{12} s^{-1}), T stands for UST temperature, and U is the pair binding energy of the order of 0.5eV. It is easy to check that at 70kHz the Eq. (1) is fulfilled at 124°C, which is close to the range of applied UST temperatures. The breaking of Fe-B pair under UST occurs when the Fe atom approaches a saddle point between two equivalent interstitial sites: in this position a colombic binding energy is substantially reduced, which promotes a dissociation of the pair components.

Capture of point defects: dislocation gettering in II-VI

UST stimulated capture of mobile defects was experimentally observed in different II-VI semiconductors (Table I).

Point defect gettering benefits mechanical, transport, and optical properties of electronic material.

The physical origin of UST gettering is a selective absorption of the ultrasound at extended crystal defects such as dislocations, grain boundaries, and precipitates. The energy of absorbed UST vibrations can be coupled with point defects and activate different defect reactions. We consider

the vibrating string model of Granato-Lucke to describe a dislocation motion stimulated by the ultrasound [19]. Within this model, a dislocation line is considered as an elastic string oscillating between pinning points. It is assumed that for zero applied stress the dislocations are straight and pinned down by the impurity particles Fig.3,a. In general, the concentration c of impurity atoms on the dislocation line is larger than the overall concentration c_0 of impurities in the lattice,

Table I. Ultrasound stimulated processes in semiconductors

Physical mechanism	Semiconductor [Ref.]
Capture of point defects	CdS [3] CdTe [4] ZnCdTe[5]
Multiplication of dislocations	GaAs, GaP[6] ZnCdTe[5] Ge/GaAs[7]
Dissolving of defect clusters and pairs	HgCdTe [8] Cz-Si [9] poly-Si films[10, 11] CdS[12] GaAs[13]
Enhanced diffusivity of point defects	Ge [14] Si [15] CdS[16]
Metastable effects	Cz-Si [9] GaAlAs[17] GaAs [18] CdS [3]

which is known as a dislocation Cottrell atmosphere.

At temperatures T high enough for diffusion to take place, the concentration can attain an equilibrium value according to

$$c=c_0 exp(Q/kT), \qquad (2)$$

where Q is Cottrell interaction energy between a dislocation and impurity atom.

If an external low stress is now applied (Fig.3, b), the loops (L_c) start to bow out until the breakaway stress is reached. At the breakaway stress (Fig.3, c), a large increase in the dislocation strain occurs. Due to this dramatic increasing of the dislocation strain in (Fig.3, c-d), the additional impurities can be swept out from the bulk and captured at the Cottrell atmosphere around the dislocation. It is suggested that both the elastic strain and electric field of charged dislocation core are the driving forces in this UST gettering mechanism, contributing to the increase of the energy Q in Eq.(2). Further increase of applied stress provides a multiplication of dislocations according to the Frank-Read mechanism (Fig.3, e). This process will be discussed in section concerning the network of misfit dislocations. Dislocation motion can be monitored by measuring the internal friction

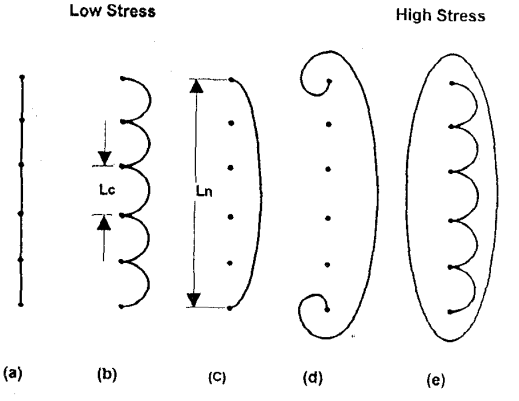

Figure 3. The successive drawings indicate schematically the bowing out of a pinned dislocation line by an increasing applied stress. As the stress increases, the loop L_c bow out until breakaway occurs. For very large stresses, the dislocations multiply according to Frank-Read mechanism.

coefficient which quantifies the value of dislocation ultrasonic damping. Internal friction study accesses the mechanical properties of a dislocation network such as density of pinning points, length of dislocation segments, and breakaway stress.

A variation of defect concentrations is ultimately reflected at the intensity change of corresponding PL lines. In Figure 4, our concern is the intensity of two exciton lines: I_1 (acceptor exciton) and I_2 (donor exciton), and the donor-acceptor line with the principal maximum at 805nm (1.54eV) The UST obviously reduces the intensity of the acceptor excitonic line (I_1) and the donor-acceptor lines while barely changing the donor excitonic line (I_2). This UST process was identified as a gettering of acceptor-type impurities: substitutional Li and Na. Similar UST results were obtained with gettering of Cu and Ag in CdTe and interstitial Cd_i and S_i in CdS [3].

The illustrative example of UST defect gettering is shown in Figure 4 as two photoluminescence spectra measured in CdTe single crystal before UST and after UST processing [4].

It was concluded, that mobile point defects can be captured effectively by a dislocation network after UST processing. The PL spectroscopy data were approved by electrical measurements using thermally-stimulated conductivity. They are in consistency with the results of internal fraction study: decreasing of the internal friction coefficient after UST was observed in CdS single crystals. This result strongly suggests that the concentration of pinned points shown in Figure 3 was increased after UST processing, confirming the model of point defect gettering.

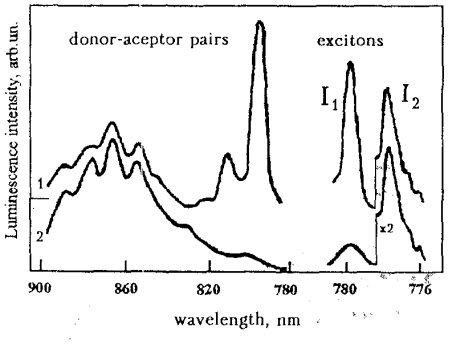

Figure 4. UST processing strongly reduces the concentration of shallow acceptors (I, line) and donor-acceptor pairs in CdTe single crystals. This is shown as two photoluminescence spectra of the same CdTe crystal measured at T=4.2K before UST (1) and after UST (2).

Multiplication of dislocations: strained Ge films on GaAs

Defect gettering can be also closely related to another important UST phenomena: generation and multiplication of dislocations. In particular, promptly engineered dislocation network can benefit electronic materials, as was suggested, by using misfit dislocations in the SiGe/Si system [20]. In fact, dislocations in the vicinity of an active region can be an excellent sink to capture residual impurities and to accomplish defect gettering. Dislocations also provide a means to release a residual undesirable stress field at the misfit boundary between film and substrate. UST generation of dislocations occurs at relatively high UST density of power and is a result of a strong plastic deformation in crystal lattice. Within a string model described previously, dislocations under strong UST stress can be released from some of its pinned points and a dislocation multiplication will occur.

This process was directly observed using transmission electron microscopy in strained heterolayers composed of 0.2 μm to 5 μm Ge films deposited at GaAs substrate [7]. By applying UST processing for 3 hours at 160kHz with the acoustic strain amplitude up to 2×10^{-4} it was found that UST promotes the glide and multiplication of existing dislocations in strained Ge/GaAs heterostructure.

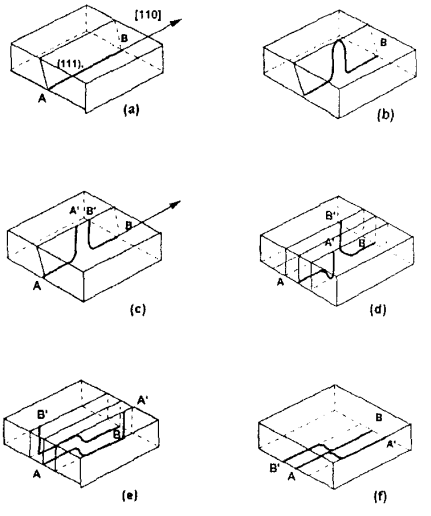

Figure 5. Schematic of consecutive stages of UST induced multiplication of the misfit dislocations at the heteroboundary between a thin film and substrate.

The following mechanism of a multiplication of misfit dislocations is schematically shown in Figure 5. Initially (Fig.5, a), a straight 60° misfit dislocation AB oriented along [110] direction is shown in the film-substrate boundary. Under the UST (Fig.5, b), the dislocation dipole is formed in the (III) glide plane. This dipole can be broken by approaching a film surface (Fig.5, c), leaving two helical sections on the dislocation configurations AA' and BB'. The misfit stresses cause these sections to glide transversely (Fig.5, d) and also in planes parallel to the original glide plane (Fig.5, e), lengthening the misfit dislocation segments and subsequently relaxing misfit stresses. When the helical segments reach the edges of the film, the final pattern of two new misfit dislocations - AA' and BB' - is designed. This elementary process of a dislocation multiplication can be repeated under UST with AA'

and BB' dislocations. Consequently, a misfit dislocation network can be engineered.

We notice that dislocations are usually considered harmful defects to a semiconductor material or device. Therefore, special precautions have to be undertaken to avoid degradation of device performance after the dislocation network is created by UST. Methods of dislocation passivation, e.g. using the atomic hydrogen from a plasma source, as described in the next section, can resolve this problem.

Dissolving of defect clusters: hydrogenation enhancement in poly-Si.

Polycrystalline silicon (poly-Si) thin films on glass or fused silica substrates are promising for thin film transistor (TFT) technology in active matrix liquid crystal displays. Compared with transistors using amorphous silicon films, poly-Si TFTs have improved operational parameters due to a substantially higher electron mobility. However, grain boundary states and interface defects in poly-Si lead to a high off-state current and affect a threshold voltage. A conventional approach to passivate these defect states and to reduce inter-grain barriers for electron transport is to apply plasma hydrogenation. The hydrogen defect passivation occurs in two steps: plasma penetration and a subsequent atomic hydrogen diffusion. Unfortunately, the diffusion of hydrogen in poly-Si is slow compared with single crystal silicon due to a trap limiting mechanism at grain boundaries, resulting in a long hydrogenation time (typically an hour at 300°C) and electrical inhomogeneity within passivated regions of poly-Si. This problem motivates a search for non-traditional approaches in order to improve hydrogenation in poly-Si films. It has appeared that the atomic hydrogen in poly-Si thin films is a specifically suitable object for UST processes [10]. Based on experiments, the mechanism of UST enhanced liberation of the atomic hydrogen from trapping states was proposed [11]. This UST effect is a "trigger" of fast hydrogen diffusion in poly-Si and ultimately provides an effective passivation of defects at grain boundaries.

For UST experiments, ultrasound vibrations were generated into 0.5 μm poly-Si films and thin-film transistors through a glass substrate using a circular 75mm diameter piezoelectric transducer. The UST transducer operated at about 25kHz resonance of radial vibrations at temperatures ranging from room temperature to 300°C. The UST effect was monitored by measurements of a sheet resistance at room temperature using the four-point-probe method. Concurrently, spatially resolved PL and nanoscale contact potential difference mapping were performed.

It was found that conventional plasma hydrogenation applied to poly-Si films reduces a sheet resistance up to one order of magnitude due to hydrogenation of grain-boundary dangling bonds. In films where plasma hydrogenation process was not completed, the additional strong reduction of resistance after UST by a factor of ***two orders*** of magnitude was observed (Fig. 6).

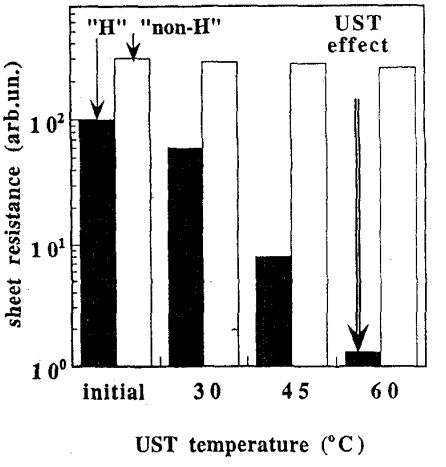

Figure 6. Effect of UST on the reduction of sheet resistance in plasma hydrogenated poly-Si thin film ("H") compared to non-hydrogenated film ("non-H"). UST parameters: acoustic strain 10^{-5} frequency 70kHz, temperature 55°C.

Important, that resistance in non-hydrogenated films was practically not changed after the same UST. Another feature of the UST effect is an improvement of resistance homogeneity.

Photoluminescence (PL) spectroscopy accesses hydrogenation monitoring in poly-Si films. The PL intensity in poly-Si is increased after hydrogenation due to passivation of non-radiative centers: dangling silicon bonds at the grain boundaries.

Spatially resolved PL mapping technique with a resolution of 100 μm was used to monitor UST changes in distribution of recombination centers.

The result is presented in Figure 7 as two histograms of exactly the same hydrogenated film area prior to and after UST. The average value of PL intensity after UST exhibits an additional 30% increase and a narrowing of the histogram half-width by a factor of two (Fig.7). This result is in the excellent agreement with the UST-induced improvement of resistance homogeneity.

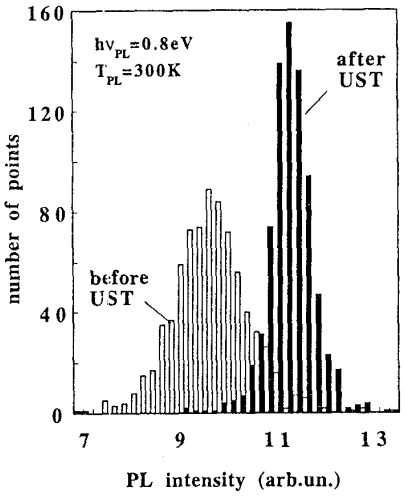

Figure 7. UST improves homogeneity of the photoluminescence intensity. PL mapping shows the increase of PL intensity and narrowing of the histogram in hydrogenated poly-Si film.

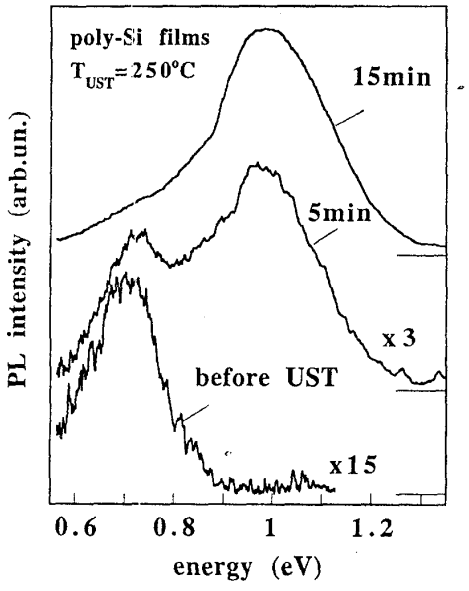

Figure 8. UST processing at 250°C for a few minutes exhibits a dramatic increase of luminescence intensity. This is due to passivation of non-radiative recombination centers with liberated atomic hydrogen.

A dramatic UST effect was found in poly-Si films recrystallized from amorphous silicon (a-Si) at 550°C which contained a mixture of a-Si and poly-Si phases. A volume ratio of crystalline to amorphous phase was quantitatively measured by Raman spectroscopy. After UST was applied to films at T_{UST}=150-280°C, noticeable changes in the PL spectrum were observed (Fig. 8).

Generally, the entire PL intensity was increased after UST. On the other hand, UST strongly activates a new broad PL band with a maximum at about 1.0 eV and a halfwidth of 0.26 eV. It is important that a dramatic enhancement of 1.0 eV band exceeding ***two orders*** of magnitude requires only a few minutes of UST processing performed at 250°C. After UST activation of luminescence is completed, the PL spectrum is entirely dominated by the 1.0 eV band as shown in Fig. 8. UST processing was performed at different temperatures between 150°C and 280°C, which allowed to evaluate the activation energy of the UST effect, E_{UST}=0.33eV.

This value is an important parameter for the suggested UST model. It is important that this UST effect is a stable one: no relaxation was observed for a few months within a temperature range from a room temperature up to 300°C.

It is known that after plasma hydrogenation the total hydrogen concentration in poly-Si films can exceed the number of non-passivated dangling bonds by as much as two orders of magnitude. Therefore, a significant "reservoir" of electrically non-active hydrogen in trapping states is available after plasma hydrogenation. It is suggested that UST promotes a release of hydrogen from traps. A physical basis of such UST hydrogen detrapping is a selective absorption of the ultrasound by grain boundaries, dislocations, and other extended crystal defects where hydrogen can reside. Being liberated from traps, hydrogen subsequently become a fast diffuser with the diffusion coefficient of crystalline Si: $D_H = 9.4 \cdot 10^{-3} \times \exp(-0.48\text{eV}/kT)$ [cm^2/sec]. In fact, the measured UST activation energy (E_{ust}=0.33eV) has a value close to the activation of H diffusion in crystalline Si (about 0.48eV). A possible reduction of this energy can be attributed to UST stimulated diffusion of the hydrogen.

The UST processing was also applied to hydrogenated poly-Si thin film transistors. The reduction of a leakage current by a factor of 10, and a shift of threshold voltage by as much as 0.5V, are consistent with the proposed model of UST enhanced hydrogenation. These experiments demonstrate a utility of UST processing for the improvement of poly-Si active-matrix displays.

Enhanced diffusion: Cr in Cz-Si

Ultrasound accelerated diffusion of point defects was unambiguously observed first in metals, and after that in semiconductor Ge and Si. UST reduces the activation energy of the diffusion process by a few tenths of an electron-volt, and by this means, it facilitates low-temperature defect reactions. This UST effect can potentially contribute in the gettering process. UST enhanced diffusion is related to the multiplication of dislocations described above. In fact, diffusion of substitutional In, Al, and Ga in germanium single crystals was accelerated via dislocation network. The mechanism is based upon the fact that point defect diffusion is accelerated along the dislocation pipe compared to that in a regular crystal.

Diffusivity of point defects can also be facilitated in a dislocation-free material such as Cz-Si wafers. According to theoretical model [21], the impurity atom absorbs the energy of nonequilibrium phonons excited by the ultrasound, and this energy increases the rate of impurity migration. Two specific factors contribute to this UST mechanism: (1) the change in population of the impurity quantum oscillator levels due to the interaction of an impurity atom with ultrasonically excited non-equilibrium phonons, and (2) the change of a probability of an impurity migration at a particular quantum level.

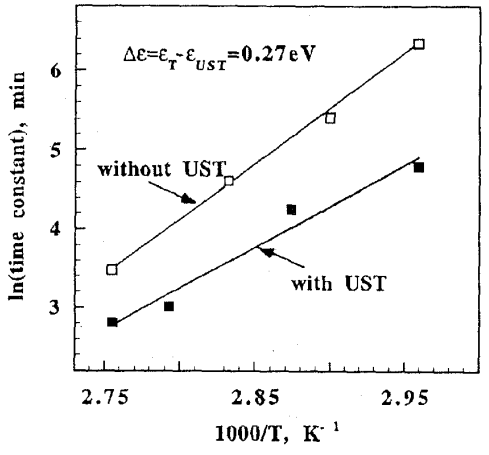

Figure 9. Ultrasound vibrations stimulate low-temperature diffusion of interstitial Cr in Cz-Si. UST reduces the activation energy of Cr diffusion to form Cr-B pairs.

Experiments were performed in p-type boron doped Cz-Si wafers co-doped with Cr at concentration from 10^{-12} to10^{-14} cm^{-3} [22]. In equilibrium, interstitial chromium atoms - Cr_i - form the nearest-neighboring Cr-B pairs which can be dissociated after 200°C annealing and quenching of Si wafer. The following low-temperature pairing kinetics of Cr_i and B is entirely controlled by Cr_i bulk diffusion, which provides a convenient method to measure low-temperature diffusivity of the chromium ions. Measured in this way the activation energy of Cr; diffusion without UST of 0.86eV is consistent with published data. It is shown that this activation energy is significantly reduced by 0.27eV under the UST (Figure 9).

Another example is revealed by the UST enhanced diffusivity of donors in CdS single crystals where the ultrasound was generated with a pulsed laser beam [16]. The effect of shallow donor gettering by dislocations was substantially enhanced and occurred within a micro-second time-frame, independent of the UST temperature between 77K and 300K. This was interpreted as an extremely low activation energy of point defect diffusivity under pulsed UST processing.

4. UST APPLICATION

In Table II we summarized the results of UST application in various semiconductor devices. The upper-limit of UST effect shows the record of UST improvement of a device parameter. Some UST effects are indeed spectacular, while the others depict just a trend to follow-up research.

Table II. Improvement of semiconductor devices using UST

Type of device (Material)	Improved parameter (Upper limit of UST effect)
Thin-film transistor (poly-Si on glass)	Leakage current (10 times lower)
	Threshold voltage (0.5V lower)
Solar cell (poly-Si)	Quantum efficiency (20% higher)
Tunnel diode (GaAs)	Current noise (4 times lower)
Photodetector (CdSe)	Dark current (100 times lower)
Integrated circuit (Si)	Current noise (2 times lower)
Light emitting diode (InGaAs, AlGaAs)	Intensity (90% higher)

To illustrate one of the UST applications, a suppression of 1/f spectral density of noise in

$Cd_{0.2}Hg_{0.8}Te$ polycrystalline material is shown in Figure 10 [22].

This material is a recognized leader among infrared detectors and this interest is motivated by commercial and military applications. Samples were cut from the n-type $Cd_{0.2}Hg_{0.8}Te$ slab containing small-angle boundaries with the density from $20cm^{-1}$ to $70cm^{-1}$. The $Cd_{0.2}Hg_{0.8}Te$ lattice is characterized by a high concentration of mobile point defects such as Hg vacancies, defect precipitates in a form of HgTe and Te inclusions, dislocations, and small-angle grain boundaries. This complicated defect system appeared to be a proper object for the UST processing. The optimal UST effect was observed at an ultrasonic frequency in the range of 10 MHz, close to the characteristic vibration frequency of individual subblocks.

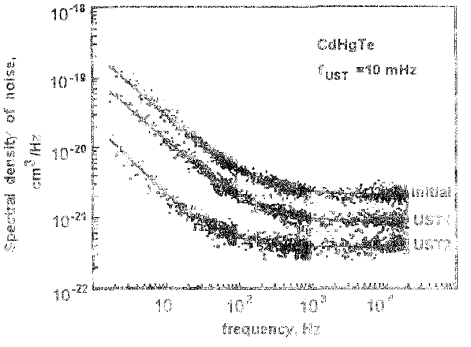

Figure 10. UST applied to CdHgTe ternary compound reduces the spectral density of 1/f noise by a factor of one order of magnitude (curve 3) compared to the initial state (curve 1). Further increasing of the UST intensity degrades the noise level to approximately initial one.

The UST was performed at room temperature increasing the UST time from a few minutes to an hour. It is imperative to know that due to an extremely complicated combination of point and extended defects in a "soft" CdHgTe lattice, the UST effect is sensitive to experimental details, and even varies between samples cut from the same polycrystalline slab possessing different densities of small-angle grains boundaries. A dramatic, one order of magnitude reduction of 1/f noise level (critical parameter of IR sensitivity) is very impressive and promising for IR applications.

5. SUMMARY AND CONCLUSIONS

We have reviewed fundamental and application issues of the UST method in various semiconductors and electronic devices: single and compound materials; crystalline, polycrystalline, and amorphous; as-grown and processed wafers. Numerous ultrasonic-controlled defect reactions were observed and explored. Examples of a significant UST effect to enhance the point defect gettering and defect passivation with atomic hydrogen exhibit a strong potential for the UST technology to be utilized as a defect engineering tool.

After a comprehensive study, UST mechanisms enabled the development of a reliable methodology and apparatus for using the UST in microelectronics and optoelectronics. Feasibility projects performed on semiconductor devices, established a statistically valid data-base for applying this technique to benefit device performance. Although the core of UST technology – a generation of the ultrasound into electronic material - is a common feature for various UST applications, a specific UST recipe has to be developed for each individual type of material or device. Such a recipe is comprised of a synergetic combination of the optimal UST parameters: temperature, amplitude, duration, and resonance frequency. Additionally, UST processing can be performed concurrently or consecutively with UV or IR light, under a pulsed electric field or laser activation, etc. This illustrates a high level of flexibility of the UST technology, its compatibility with different stages of a device fabrication, and an easy adjustment to a particular device problem.

REFERENCES

1. *I. V. Ostarovskii and V. N. Lysenko, Sov.Phys.Solid State, vol. 24, p.1206, 1982.*
2. *J. Lagowski, P. Edelman, M. Dexter and W. Henley, Semicon. Sci. Technol., vol.7, p. A185, 1992.*
3. *A. P. Zdebskii, N. V. Mironyuk, S. S. Ostapenko, A. U. Savchuk, and M. K. Sheinkman, Sov.Phys.Semicond., vol.20, p.1167,1986.*
4. *V. N. Babentsov, S. I. Gorban', I. Ya. Gorodetckii, N. E. Korsunskaya, I. M. Rarenko, and M. K. Sheinkman, Sov.Phys.Semicond., vol.25, p.749,1991.*
5. *S. G. Garyagdiev, I. Ya. Gorodetckii, B. R. Dzhumaev, N. E. Korsunskaya, I. M. Rarenko, and M. K. Sheinkman, Sov.Phys.Semicond., vol.25, p.248,1991.*
6. *D. Klimm, B. Tippelt, P. Paufler, and P. Haasen, Phys.Stat.Sol. (a), vol.138, p.517,1993.*
7. *V. F. Britun, N. Ya. Gorid'ko, V. L. Korchnaya, G. N. Semyonova, M. Ya. Skorohod, Yu. A. Thorik, L. S. Khazan, and M. K. Sheinkman, Sov.Phys. Solid State, vol.33, p.1317, 1991.*

8. *P. I. Baranskii, A. E. Belyaev, S. M. Komirenko, and N. V. Shevcenko, Sov. Phys. Solid State, vol.32, p.1257, 1990.*
9. *S. Ostapenko and R. Bell, J.Appl.Phys., vol.77, p.5458,1995.*
10. *S. Ostapenko, L. Jastrzebski, J. Lagowski, and R. K. Smeltzer, Appl.Phys. Lett., vol.68, p.2873, 1996.*
11. *J. Koshka, S. Ostapenko, T. Ruf, and J. M. Zhang, Appl. Phys. Lett., vol.68, p.2537, 1996.*
12. *V. L. Gromashevskii, V. V. Dyakin, E. A. Sal'kov, S. M. Sklyarov, N. S. Khilimova, Ukr.Fiz.Zhurnal, vol.29, p.550,1984.*
13. *A. Makosa, T. Wosinski, and Z. Witczak, Acta Physica Polonica A, vol.84, p.653,1993.*
14. *V. P. Grabchak and A. V. Kulemin, Sov. Phys. Acoust., vol.22, p.475,1976.*
15. *V. D. Krevchik, R. A. Muminov.and A. Ya. Yafasov, Phys. Stat. Sol. (a), vol.63, p.K159,1981.*
16. *L. V. Borkovskaya, B. R. Dzhumaev, I. A. Drozdova, N. E. Korsunskaya, I. V. Markevich, A. F. Singaevskii, and M. K. Sheinkman, Sov. Phys. Solid State, vol.37, p.1511, 1995.*
17. *E. Belyaev, H. J. von Bardeleben, and M. F. Fille, E. I. Oborina, Yu. S. Ryabchenko, A. U. Savchuk, M. K. Sheinkman, Material Science Forum, vol.143-147, pt.2, p.1057,1994.*
18. *I. A. Buyanova, S. S. Ostapenko, M. K. Sheinkman, and M. Murrikov, Semicond. Sci. Technol., vol.9, p.158,1994.*
19. *A. V. Granato and K. Lucke, "The vibrating string model of dislocation damping", in Physical Acoustics, ed.by W.P.Mason, vol.4A, p.225,1966.*
20. *F. Shimura, Semiconductor silicon crystal technology. San Diego, CA: Academic Press, Inc., 1989.*
21. *R.E. Bell, S. Ostapenko and J. Lagowski, in "Defect and impurity engineered semiconductors and devices", Material Research Society, Pittsburg, PA 1995, p.647.*
22. *Ya. M. Olikh and Yu. N. Shavlyuk, Sov. Phys. Solid State, vol.38, p.1835, 1996.*